Electronic Journal of Biotechnology 67 (2024) 23–33

Contents lists available at ScienceDirect

Electronic Journal of Biotechnology

journal homepage: www.elsevier.com/locate/ejbt

Research article

Long non-coding RNA KCNQ1 opposite strand/antisense transcript 1, a potential biomarker for glaucoma, accelerates glaucoma progression via microRNA-93-5p/Homeobox box 3 axis ☆,☆☆

ZhaoLian Xie *, Hui Wang, LinLin Liu, HaiQing Zhang, Jing Liu

Department of Ophthalmology, The First Affiliated Hospital of Gannan Medical College, Ganzhou City, Jiangxi Province 341000, China

GRAPHICAL ABSTRACT

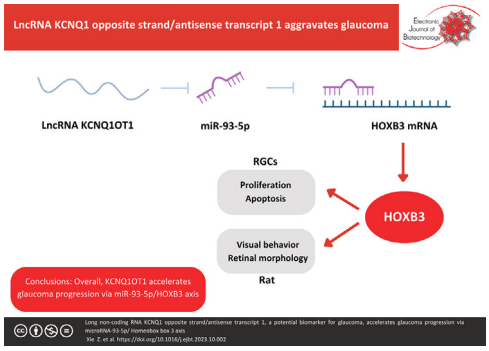

ARTICLE INFO

Article history:
Received 10 July 2023
Accepted 12 October 2023
Available online 29 October 2023

Keywords:
Antisense transcript
Biomarkers
Glaucoma
Homeobox box 3
Long non-coding RNA
MicroRNA-93-5p
Neurodegenerative disease
Ophthalmic testing
Opposite strand
Retinal ganglion cells
Risk factor

ABSTRACT

Background: Glaucoma is marked by retinal neuron death in the ganglion cell layer, leading to irreversible vision loss. Aberrant long non-coding RNA (lncRNA) expression is associated with glaucoma. The study was to explore the latent molecular mechanism of lncRNA KCNQ1 opposite strand/antisense transcript 1 (KCNQ1OT1) in N-methyl-D-aspartate (NMDA)-stimulated glaucoma.
Results: The data demonstrated that KCNQ1OT1 expression was elevated in glaucoma patients, serving as a diagnostic biomarker of glaucoma. Rats injected with NMDA developed visual loss and retinopathy and expressed high KCNQ1OT1. After treating retinal ganglion cells (RGCs) with NMDA, cell proliferation was suppressed and apoptosis was augmented. Silenced KCNQ1OT1 or HOXB3 or elevated miR-93-5p alleviated NMDA-induced suppression of RGC growth. KCNQ1OT1 mediated miR-93-5p expression by targeting homeobox box 3 (HOXB3). The protection of silenced KCNQ1OT1 in NMDA-treated RGCs was turned around by elevated HOXB3.
Conclusions: Overall, KCNQ1OT1 accelerates glaucoma progression via miR-93-5p/HOXB3 axis.
How to cite: Xie ZL, Wang H, Liu LL, et al. Long non-coding RNA KCNQ1 opposite strand/antisense transcript 1, a potential biomarker for glaucoma, accelerates glaucoma progression via microRNA-93-5p/Homeobox box 3 axis. Electron J Biotechnol 2024;67 . https://doi.org/10.1016/j.ejbt.2023.10.002.

Peer review under responsibility of Pontificia Universidad Católica de Valparaíso
☆ Audio abstract available in Supplementary material.
* Corresponding author.
E-mail address: xiezl_1783@outlook.com (Z. Xie).

https://doi.org/10.1016/j.ejbt.2023.10.002

1. Introduction

Glaucoma is a neurodegenerative disease characterized by progressive loss of retinal ganglion cells (RGCs) and axons, leading to visual field defects and irreversible vision loss [1]. Recently, the incidence of glaucoma has been escalating worldwide [2]. Unfortunately, the early symptoms of glaucoma in numerous patients are not distinct, and they must be detected early by ophthalmic testing. As reported, intraocular pressure (IOP) is the only modifiable risk factor for glaucoma [3]. Currently, treatments aiming to reduce IOP are based on external drugs and laser therapy, and surgical intervention is required when necessary [4]. Though with dramatic advances, there are no imperative measures that can completely prevent glaucoma occurrence and reverse its progression. Additionally, glaucoma is primarily diagnosed by optic nerve examination and ultrasonic biological microscopy currently, which are not only expensive but susceptible to the subjective judgment of the operator. Consequently, it is urgent to develop brand-new diagnostic biomarkers [5].

The genomes of many species are widely transcribed, producing many long non-coding Rnas (LncRNAs) [6]. LncRNA is an endogenous non-coding RNA with a length of over 200 nucleotides, lacking or having limited protein-coding potential and being available to modulate protein formation via different mechanisms [7]. Numerous studies have elucidated that lncRNAs participate in diversified biological processes and modulate genes through epigenetics, translation, and transcription, thereby impacting cell proliferation, apoptosis, immune response, and oxidative stress [8]. LncRNA-MALAT1 mediates RGC apoptosis in glaucoma rats via the phosphatidylinositol 3-kinase (PI3K)/Akt signaling pathway [9]. LncRNA KCNQ1 opposite strand/antisense transcript 1 (KCNQ1OT1) expression is aberrant in solid tumors and has been broadly explored as a prognostic biomarker [10]. A foregoing study has clarified that KCNQ1OT1 expression is elevated in the anterior lens capsule and accelerates hydrogen peroxy-stimulated lens epithelial cell apoptosis and oxidative stress via modulating miR-223-3p/BCL2L2 axis [11]. Also, KCNQ1OT1 knockdown can promote the migration of human corneal epithelial cells and accelerate the healing of corneal wounds [12]. Nevertheless, the expression and role of KCNQ1OT1 in glaucoma remain unknown.

In this study, KCNQ1OT1 in glaucoma tissue specimens, N-methyl-D-aspartate (NMDA)-stimulated glaucoma rats, and RGC models were primarily explored, and its function in IOP, the retina of glaucoma rats and proliferation and apoptosis of RGCs *in vitro* was assessed.

2. Materials and methods

2.1. General information

A total of 50 glaucoma patients diagnosed in The First Affiliated Hospital of Gannan Medical College were enrolled, including 27 males and 23 females with an average age of 51.19 ± 1.33 years. During the same term, 50 healthy volunteers admitted to The First Affiliated Hospital of Gannan Medical College for physical examination served as controls. The diagnostic criteria for glaucoma were as follows [13]: (1) history of IOP higher than 21 mm Hg, (2) glaucomatous optic disc damage (vertical cup-to-disc ratio > 0.7, and/or interocular asymmetry of cup-to-disc ratio > 0.2, and/or focal rim notching), (3) corresponding visual field defect. All glaucoma patients underwent serial ophthalmologic examinations by experienced glaucoma specialists. The mean defect of the entire visual field was detected by a Humphrey Field Analyzer (Carl Zeiss Meditec, CA, USA). In addition, retinal nerve fiber layer thickness was detected by depth imaging optical coherence tomography (Atlantis, DRI OCT-1; Topcon, Tokyo, Japan). Medications used in patients with glaucoma were recorded. Exclusion criteria: Patients complicated with other eye diseases; Patients with pregnancy or lactation; Patients complicated with other malignant tumors; Patients with severe immune system diseases; Patients with severe hepatic and renal insufficiency. All patients and their families agreed to participate in this study and were authorized by the Ethics Committee of The First Affiliated Hospital of Gannan Medical College (Approval number is GN2091-20153).

2.2. Test indexes

Venous blood (5 mL) was drawn on an empty stomach, anticoagulated with heparin, and centrifuged at 3000 rpm. Serum homocysteine (Hcy) was detected by an automatic immunochemiluminescence analyzer (Abbott, USA, Axmy), serum Pigment epithelium-derived factor (PEDF) was assessed by an automatic biochemical analyzer (Beckman Coulter, USA, Uicel Dxc800), while serum interleukin (IL)-12 and IL-4 were measured by enzyme-linked immunosorbent assay kits (Lenton Bioscience Co., Shanghai, China) [14].

2.3. Experimental animals

Sprague-Dawley (SD) rats (male, 200-250 g, 8-12 weeks) from Nanjing Junke Bioengineering Co., Ltd. were fed in separate cages under standard laboratory conditions with free food and water in a 12-h light/dark cycle. All SD rats were normal in ophthalmology and systemic tests and fed for one week. Animal experiments were carried out in line with national regulations and authorized by the Experimental Animal Ethics Committee of The First Affiliated Hospital of Gannan Medical College (Approval number is GN2091-20153).

2.4. Construction of glaucoma rat model

A glaucoma rat model was established by NMDA-stimulated RGC death [15]. Shortly, the rats were anesthetized by an intraperitoneal injection of a mixture of 80 mg/kg ketamine and 12 mg/kg toluene thiazide (Ilium Troy Laboratories, PL, Australia). Deliquescent NMDA with 0.1 M phosphate-buffered saline (PBS) at 160 nmol concentration was injected into binoculars vitreous bodies, and then, polymyxin and neomycin ointment were applied. SD rats were divided into the Sham group and the NMDA group. On d 0: rats in the sham group were injected with PBS into the vitreous while those in the NMDA group were injected with NMDA. From d 1 to d 3, 6 rats in the NMDA group were euthanized each day, and their retinas samples were collected for reverse transcription quantitative polymerase chain reaction (RT-qPCR). On d 4, visual behavior tests and intraocular pressure measurements were performed on the remaining 6 rats in the NMDA and Sham groups, and rats were euthanized to collect retina samples for hematoxylin-eosin (HE) staining, TdT-mediated dUTP-biotin nick end-labeling (TUNEL) staining, and RT-qPCR.

2.5. Lentivirus intervention

The glaucoma rats were randomly divided into the NMDA + sh-NC group and NMDA + sh-KCNQ1OT1 group. Rats were injected intravitreally with shRNA lentiviral vectors targeting KCNQ1OT1. After 4 d, the rats underwent visual behavior tests and intraocular pressure measurements and then were euthanized by inhalation of excess carbon dioxide, and the retinas were extracted for HE staining, TUNEL staining, and RT-qPCR detection. These lentiviral vectors were prepared by GenePharma.

2.6. Visual behavior test

A dark lightbox (Metronet Technology, Hong Kong, China) consisted of a dark room (0.3 m × 0.5 m × 0.5 m) illuminated by infrared light and a relatively white room (0.5 m × 0.5 m × 0.5 m) illuminated by bright white light. There was a 10 cm × 12 cm hole between the two rooms to allow the rats to walk freely from one room to another. A camera connected to Noldus recorders and monitors (German) was employed to capture the movement of rats, and the movement time was counted by Noldus EthoVision XT 8.0 software [16].

2.7. IOP measurement

IOP measurement was performed using a rebound tonometer (TonoLAB). All measurements were performed at the same time in the morning, and six automatic average measurements were considered one record.

2.8. HE staining

Retinal tissues were soaked with 10% formalin, followed by dehydration with alcohol, immersion in xylene, and paraffin embedding. Then, 4-μm sections were placed in an oven at 60°C, dehydrated in gradient alcohol (70%, 80%, 90%, 95%, 100%), and cleared in xylene. Then, the sections were stained with hematoxylin (Beijing Solarbio Science & Technology), decolorized with 0.7% hydrochloric acid ethanol, and incubated with eosin solution. Then, after dehydration with gradient alcohol (70%, 80%, 90%, 95%, 100%) and clearance in xylene, the sections were sealed with neutral gum. Ultimately, the retinal sections were observed with an optical microscope (Olympus, Japan). The thickness of ganglion cell layer (GCL) and inner plexus layer were measured by SEIPS image analyzer [17].

2.9. TUNEL

After fixation with 4% paraformaldehyde, retinal tissues were incubated with PBS containing 0.1% Triton X-100, blocked with 3% H_2O_2, and supplemented with 50 μL TUNEL. TUNEL reaction was observed after adding diaminobenzidine (Sigma-Aldrich). Under an optical microscope, the number of TUNEL-positive cells was calculated and analyzed using IMAGE J software.

2.10. Cell culture

Retinal tissue isolated from rat eyeballs with 0.125% trypsin-ethylene diamine tetraacetic acid (EDTA) and 15 U/mL papain solution (Worthington, NJ, USA) was centrifuged at 1000 r/min, resuspended in Dulbecco's Modified Eagle Medium (DMEM), and incubated with rat anti-mouse Thy 1.1 antibody (1:50, Abcam, USA). After rinsing with PBS, the cells were detached with 0.125% trypsin, added with DMEM complete medium to terminate detachment, and centrifuged at 1000 r/min. Next, RGCs were grown in a petri dish coated with poly-D-Lysine and treated with NMDA at concentrations of 50, 100, and 150 μmol/L [18].

2.11. Cell transfection

RGCs were seeded with a density of 1×10^5 in 24-well plates and added with 500 μL antibiotic-free medium. When cell confluence reached 50-70%, transfection of sh-KCNQ1OT1, sh-negative control (NC), miR-93-5p mimic, mimic NC, si-Homeobox box 3 (HOXB3), si-NC, sh-KCNQ1OT1 + oe-HOXB3, and sh-KCNQ1OT1 + oe-NC (RiboBio, Guangzhou, China) was performed based on Lipofectamine 2000 (11668-019, Invitrogen, Carlsbad, CA, USA).

Table 2
Clinicopathological information.

Factors	Normal (n = 50)	Glaucoma (n = 50)	*P*
Gender			1.000
Male	27	26	
Female	23	24	
Age (years)			1.000
51 or less	22	23	
More than 51	28	27	
BMI (kg/m^2)			1.000
23 or less	29	28	
More than 23	21	22	
History of smoking			0.546
Yes	20	24	
No	30	26	
Types			0.689
Open-angle	28	25	
Angle-closure	22	25	
PEDF (pg/mL)	16.8 ± 2.4	9.6 ± 1.2	<0.001
Hcy (mmol/L)	5.8 ± 1.4	19.5 ± 3.0	<0.001
IL-12 (pg/mL)	135.6 ± 18.3	92.2 ± 12.8	<0.001
IL-4 (pg/mL)	181.5 ± 25.0	255.4 ± 30.6	<0.001

Table 1
Primer sequences.

Genes	Sequences
KCNQ1OT1 (human)	F: 5'-GTTGGCGAGAGTTTCCAGGA-3'
	R: 5'-CGCGCACACTAGCATCTTTC-3'
KCNQ1OT1 (rat)	F: 5'-CCCAGAAATCCACACCTCGG-3'
	R: 5'-TCCTCAGTGAGCAGATGGAGA-3'
miR-93-5p	F: 5'-GCAAAGTGCTGTTCGTGC-3'
	R: 5'-AGTGCAGGGTCCGAGGTATT-3'
miR-93-5p RT sequence	5'-GTCGTATCCAGTGCAGGGTCCGAGGTATTCGCACTGGATACGACCTACCT-3'
HOXB3	F: 5'-TTCCAGAACCGTCGCATGAA-3'
	R: 5'-GGGGTCATGGAGTGTAAGGC-3'
Bcl-2	F: 5'-ATCCAGGACAACGGAGGCTG-3'
	R: 5'-CAGATAGGCACCCAGGGTGA-3'
Bax	F: 5'-GATCGAGCAGGGCGAATG-3'
	R: 5'-CATCTCAGCTGCCACTCG-3'
U6	F: 5'-CGCTTCGGCAGCACATATAC-3'
	R: 5'- AAATATGGAACGCT-TCACGA-3'
GAPDH	F: 5'- ACCCAGAAGACTGTGGATGG-3'
	R: 5'- GGAGACAACCTGGTCCTCAG-3'

Table 3
Ophthalmological examination and medication information.

Characteristics	Normal (n = 50)	Glaucoma (n = 50)
IOP (mm Hg)	13.4 ± 2.4	23.2 ± 6.8
MD (dB)	N/A	−15.1 ± 12.4
RNFLT (μm)	N/A	58.2 ± 16.8
Number of drugs	0 ± 0	1.8 ± 0.9

2.12. RT-qPCR

Total RNA was extracted from serum, rat retinal tissue, or RGCs by TRIzol reagent (Invitrogen), and reverse transcription was done by PrimeScript™ RT Reagent Kit (RR037A, Takara) for mRNA or by miScript Reverse Transcription Kit (218061, Qiagen) for miRNA. Subsequently, RT-qPCR analysis of mRNA and miRNA was performed by SYBR® Premix Ex TaqTM II (RR820A, Takara) and miScript SYBR-Green PCR Kit (218073, Qiagen) in the 7900HT Fast Real-Time PCR System (Thermo Fisher Scientific), respectively. Glyceraldehyde-3-phosphate dehydrogenase (GAPDH) and U6 were loading controls, and relative expression was calculated by $2^{-\Delta\Delta Ct}$. Synthesized primers (Table 1) were obtained (Sangon Biotech Co., Ltd., Shanghai).

2.13. Western blot

Total protein was extracted through radioimmunoprecipitation assay lysis buffer solution (Beyotime, Shanghai, China). Protein concentration was assessed by the bicinchoninic acid kit (Beyotime). Proteins were separated by 10% sodium dodecyl sulfate-polyacrylamide gel electrophoresis and electroblotted onto the polyvinylidene fluoride membrane. After blocking with 5% bovine serum albumin solution, the membrane was incubated with primary antibodies HOXB3 (PA5-103890, 1:1000, Invitrogen Antibodies), Bcl-2 (ab32124, 1:1000, Abcam), Bax (ab32503, 1:1000, Abcam), and GAPDH (ab8245, 1:1000, Abcam) and further detected with the corresponding goat anti-rabbit Immunoglobulin G secondary antibody (1:2000). Ultimately, the signal was observed using enhanced chemiluminescence reagents, and data quantification was performed through ImageJ software (Bio-Rad, USA).

2.14. Cell viability detection

RGCs were seeded in 96-well plates (2×10^5/well) and cultured in a humidified incubator. Then, 10 μL 3-(4, 5-dimethylthiazol-2-

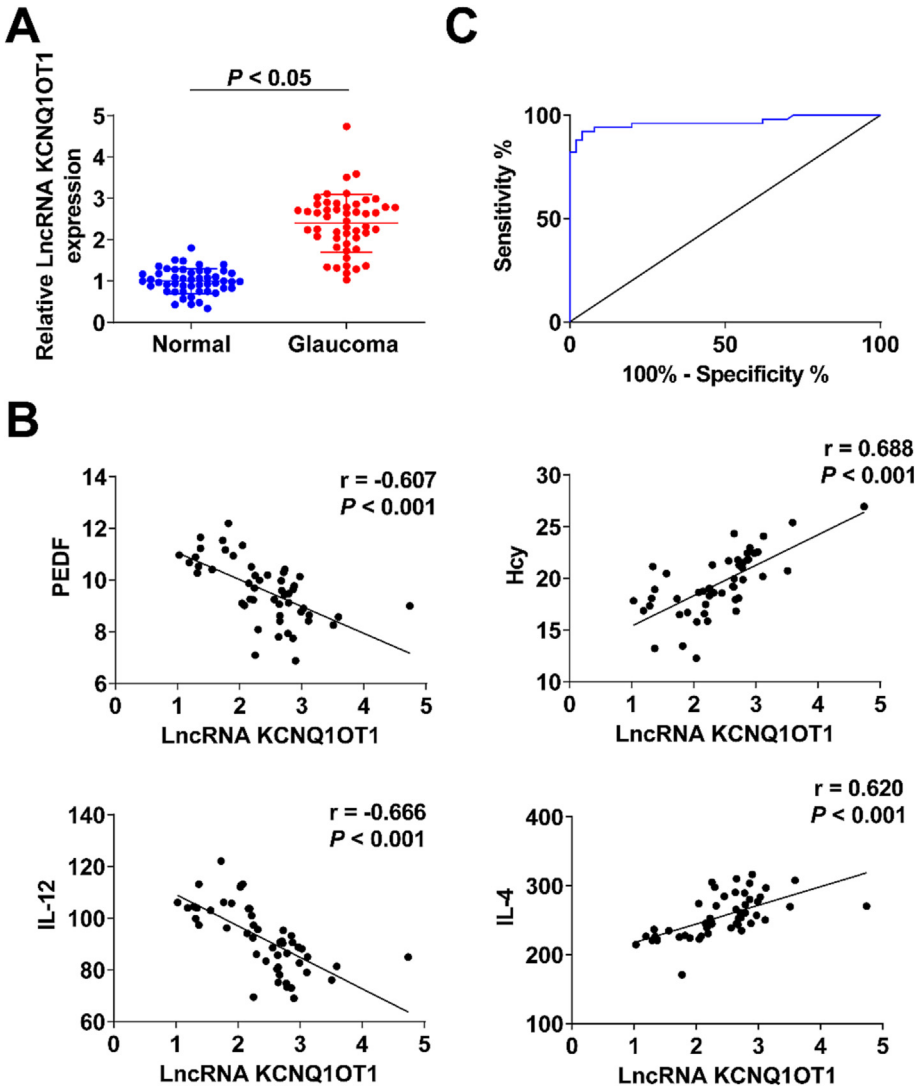

Fig. 1. KCNQ1OT1 is elevated in glaucoma patients and is a latent biomarker of glaucoma with good diagnostic value. (A) RT-qPCR test of KCNQ1OT1 in glaucoma patients; (B) Association of KCNQ1OT1 with clinicopathological indexes; (C) ROC curve diagnosis of glaucoma. The data in the figure are all measurement data in the form of mean ± SD.

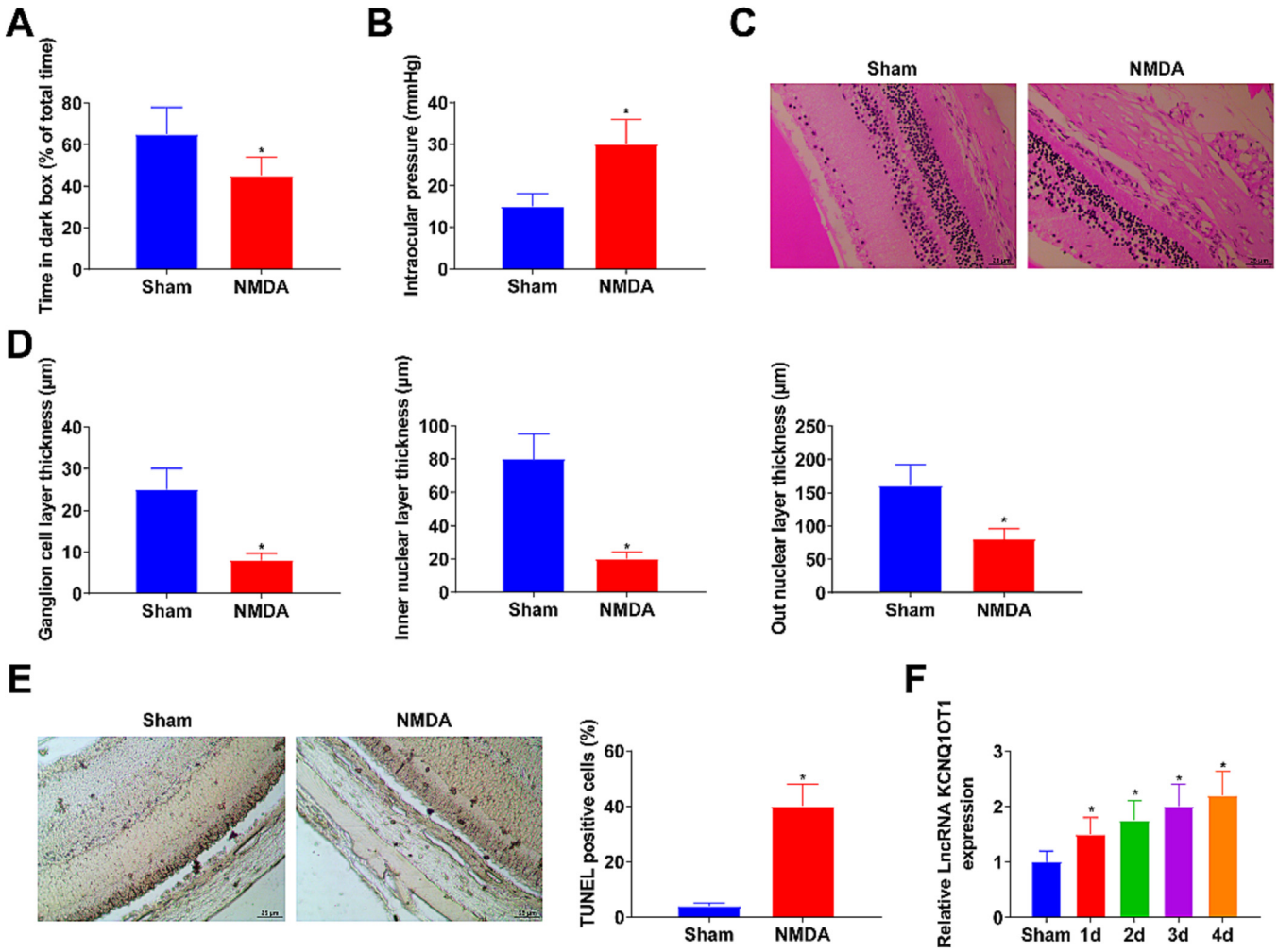

Fig. 2. KCNQ1OT1 in rats' retina is elevated after intravitreal injection of NMDA. (A) Visual behavior test; (B) Intraocular pressure measurement; (C-D) HE staining observation of retinal morphology in glaucoma rats; (E) TUNEL staining test of RGCs apoptosis in glaucoma; (F) RT-qPCR test of KCNQ1OT1 in rats injected with NMDA. The data in the figure are all measurement data in the form of mean ± SD. * vs. the Sham, $P < 0.05$.

yl)-2, 5-diphenyltetrazolium bromide (MTT) solution was added to each well, and dimethyl sulfoxide (Sigma Aldrich) was added later. Measurement of absorbance at 490 nm was performed on a spectrophotometer.

2.15. Cell proliferation test

In 96-well plates, 1,000 cells/well were serum-starved for 24 h, labeled with 5-ethynyl-2'-deoxyuridine (EdU), and detected with the Click-it assay kit (Life Technologies). At least four fields were photographed (Leica Microsystems, Wetzlar, Germany) and analyzed by ImageJ software (National Institutes of Health, Bethesda, MD) to determine the percentage of cells in the S phase.

2.16. Flow cytometry

Detachment of RGCs was implemented using trypsin free of EDTA. The cell culture fluid was centrifuged at 1,000 g to remove the supernatant, and the collected RGCs were centrifuged at 200 g, re-suspended in the binding buffer, and incubated with 5 μL Annexin V-fluorescein isothiocyanate (FITC). After centrifugation at 200 g, the supernatant was discarded and RGCs were treated with 200 μL Annexin V-FITC binding buffer, stained with 5 μL propidium iodide, and detected on a flow cytometer (Becton Dickinson, USA).

2.17. The luciferase activity assay

Starbase software predicted the target sites of miR-93-5p and KCNQ1OT1 or HOXB3. Wild-type (WT) and mutant-type (MUT) reporter plasmids of KCNQ1OT1 (KCNQ1OT1-WT/MUT) and HOXB3 (HOXB3-WT/MUT) were produced (GenePharma, Shanghai, China). When the cells reached 70% confluence, co-transfection of the synthesized reporter plasmid with miR-93-5p mimic or NC mimic was conducted with Lipofectamine 2000 (Invitrogen). After 48 h of cell transfection, measurement of luciferase activity was implemented.

2.18. Statistical methods

Statistical analysis of experimental data was performed using SPSS 18.0 software. Chi-square test was applied to compare enumeration data. Measurement data were displayed as mean ± standard deviation (SD). The two-group comparison adopted t test. Pearson analysis was used for correlation analysis. Receiver operating characteristic (ROC) curve was drawn to analyze the diagnostic value of KCNQ1OT1 in glaucoma, and multivari-

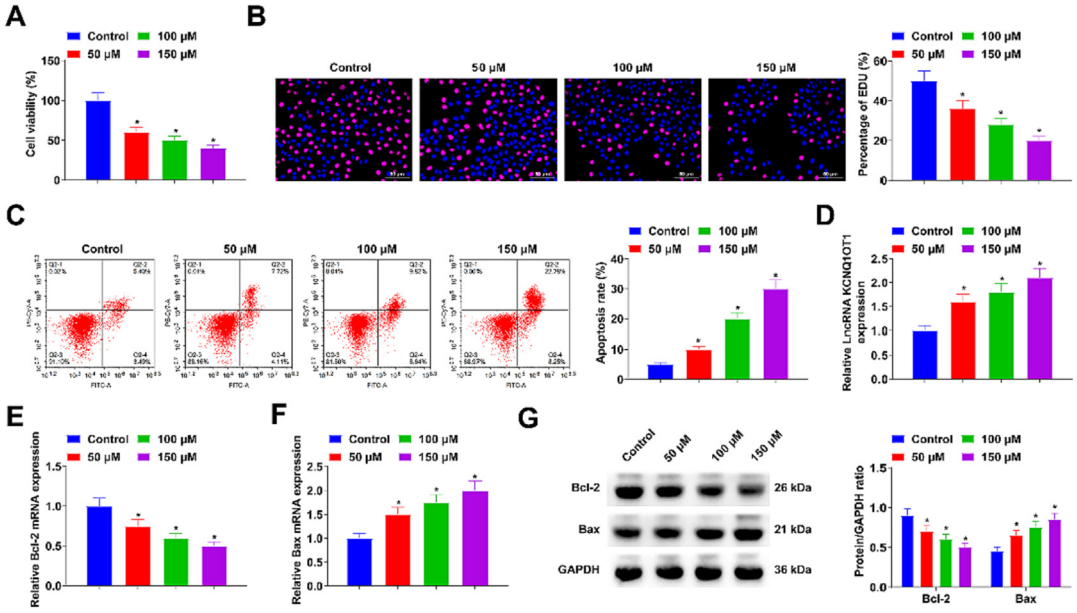

Fig. 3. NMDA restrains the growth of RGCs *in vitro*. (A) MTT test of cell viability; (B) EdU detection of cell proliferation; (C) Flow cytometry examination of cell apoptosis; (D) RT-qPCR examination of KCNQ1OT1 in NMDA-treated RGCs; (E-G) RT-qPCR and Western blot test of Bcl-2 and Bax. The data in the figure are all measurement data in the form of mean ± SD. * vs. the Control, $P < 0.05$.

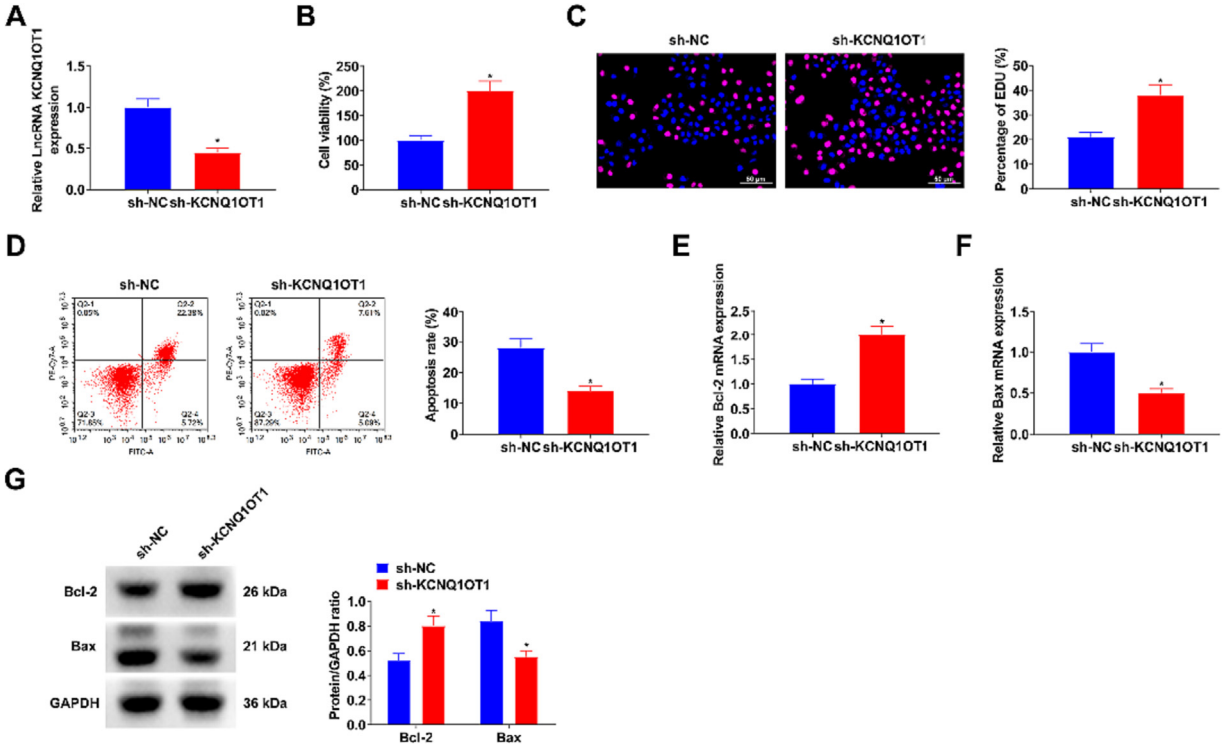

Fig. 4. Silenced KCNQ1OT1 is available to alleviate the repression of NMDA on RGCs growth. (A) RT-qPCR test of KCNQ1OT1 in RGCs after silencing KCNQ1OT1; (B) MTT examination of cell viability; (C) EdU test of cell proliferation; (D) Flow cytometry test of cell apoptosis; (E-G) RT-qPCR and Western blot detection of Bcl-2 and Bax. The data in the figure are all measurement data in the form of mean ± SD. * vs. the sh-NC, $P < 0.05$.

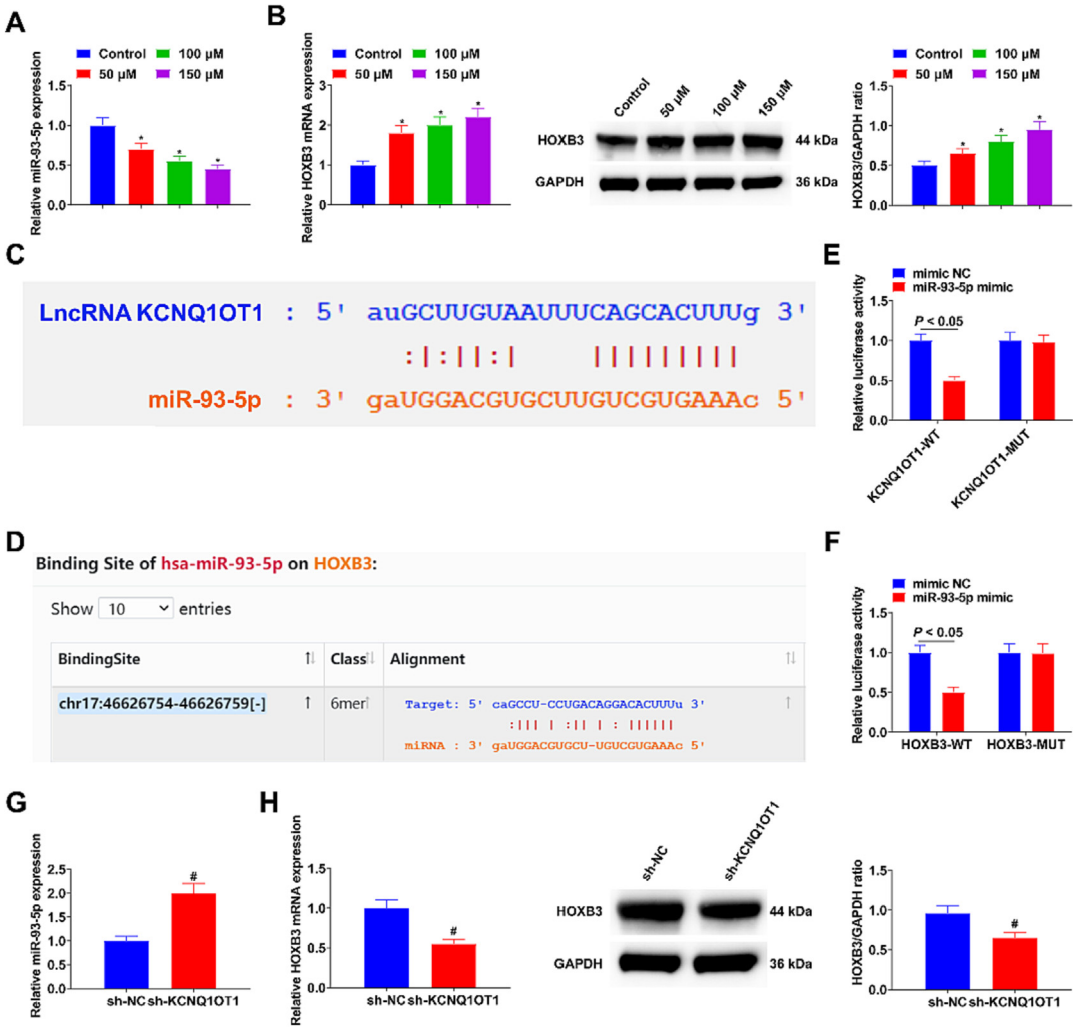

Fig. 5. KCNQ1OT1 modulates HOXB3 via miR-93-5p. (A-B) RT-qPCR and Western blot examination of miR-93-5p and HOXB3 in NMDA-treated RGCs; (C-D) Bioinformatics sites forecast of the binding sites of KCNQ1OT1 or HOXB3 and miR-93-5p; (E-F) The luciferase activity assay verification of the targeting of KCNQ1OT1 or HOXB3 with miR-93-5p; (G-H) RT-qPCR and Western blot detection of miR-93-5p and HOXB3 after silencing KCNQ1OT1. The data in the figure are all measurement data in the form of mean ± SD. * vs. the Control, $P < 0.05$; # vs. the sh-NC, $P < 0.05$.

ate Logistic regression was to analyze disease risk factors. $P < 0.05$ was accepted as indicative of distinct differences.

3. Results

3.1. Clinicopathological information on glaucoma patients

No distinct differences were presented in gender, age, and body mass index (BMI) of glaucoma patients and healthy volunteers, while serum PEDF and IL-12 contents were declined, and serum Hcy and IL-4 contents were elevated in glaucoma patients (Table 2). In addition, ophthalmological examinations revealed elevated IOP and visual field defects in patients with glaucoma (Table 3).

3.2. KCNQ1OT1 is elevated in glaucoma patients and is a latent biomarker of glaucoma with diagnostic value

Detection of KCNQ1OT1 in glaucoma patients was performed, elucidating that KCNQ1OT1 was elevated in glaucoma patients (Fig. 1A), and KCNQ1OT1 was negatively associated with PEDF and IL-12 contents, and was positively associated with Hcy and IL-4 contents (Fig. 1B). Additionally, it was discovered that the area under the curve (AUC) was 0.965 (Fig. 1C). All in all, KCNQ1OT1 was elevated in glaucoma patients and was a latent biomarker of glaucoma with a diagnostic value.

3.3. KCNQ1OT1 in rats' retina is elevated after intravitreal injection of NMDA

To further explore KCNQ1OT1's action in glaucoma progression, the construction of a glaucoma rat model was performed via intravitreal injection of NMDA. On d 4 after vitreous injection of NMDA, visual behavior tests and IOP measurements were performed. Visual behavior test aimed to examine whether a glaucoma model was established to represent glaucoma in rats. Rodents have a natural habit of avoiding light, and mice with degraded retinal photoreceptor cells cannot perceive light [19]. Visual behavior tests clarified that rats in the NMDA group stayed less time (Fig. 2A), illuminating that the NMDA impaired visual function. IOP measurement results elaborated that NMDA elevated IOP in rats (Fig. 2B). Retinal morphology of glaucoma rats was observed by HE staining, showing that after NMDA treatment, retinal layers were thinned, accompanied by reduced number of RGCs, vacuolization and thinning of GCL, inner and outer nuclear

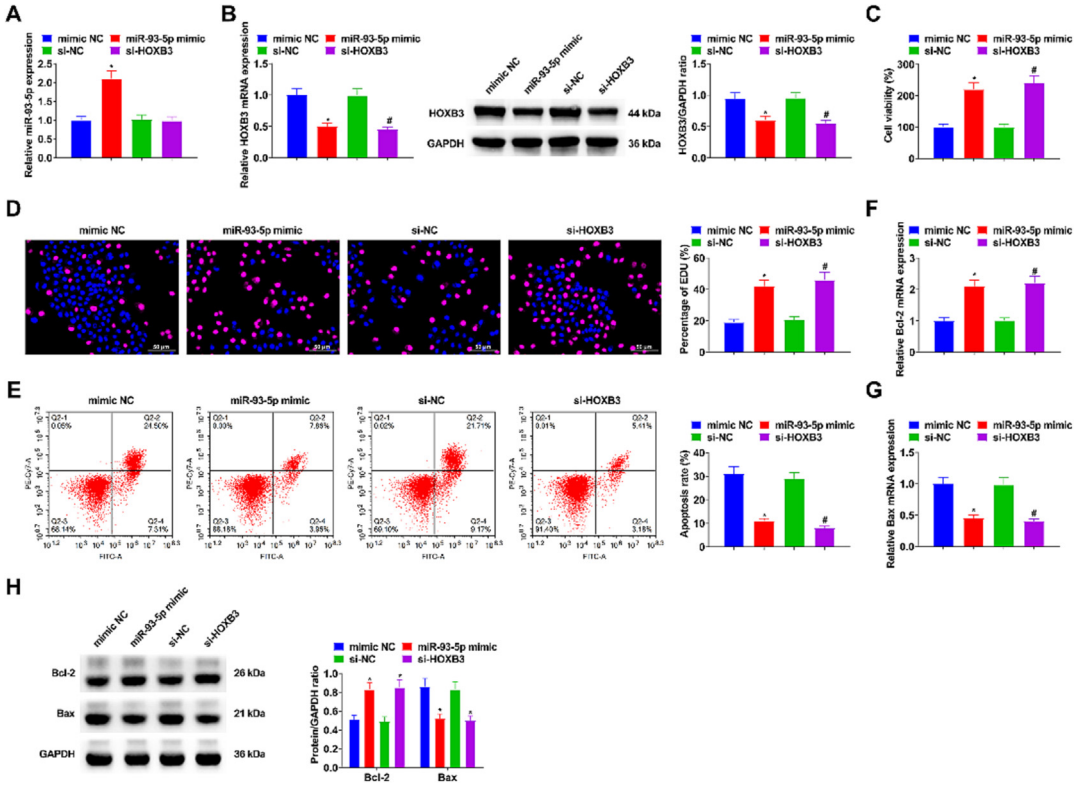

Fig. 6. Elevated miR-93-5p or silenced HOXB3 is available to alleviate the repression of NMDA on RGCs growth. (A-B) RT-qPCR or Western blot examination of miR-93-5p and HOXB3 in RGCs after intervention of miR-93-5p or HOXB3; (C) MTT test of cell viability; (D) EDU detection of cell proliferation; (E) Flow cytometry test of cell apoptosis; (F-H) RT-qPCR and Western blot test of Bcl-2 and Bax. The data in the figure are all measurement data in the form of mean ± SD. * vs. the mimic NC, $P < 0.05$; # vs. the si-NC, $P < 0.05$.

layers (Fig. 2C-D). Examination of RGC apoptosis in glaucoma was done with TUNEL staining, demonstrating that NMDA augmented RGC apoptosis of rats (Fig. 2E). It was also discovered that NMDA gradually induced the expression of KCNQ1OT1 (Fig. 2F), indicating that KCNQ1OT1 exerted a critical role in glaucoma progression. In addition, down-regulation of KCNQ1OT1 improved visual impairment in glaucoma rats (**Fig. S1A-F**).

3.4. NMDA represses RGC growth and stimulates cell apoptosis in vitro

To assess the influence of NMDA concentration on RGCs, cell proliferation was detected by MTT assay and EdU assay. With the increase in NMDA concentration (0 to 150 μM), the proliferation and anti-apoptosis of RGCs were gradually limited (Fig. 3A-C). KCNQ1OT1 in RGCs was gradually elevated with the increase of NMDA concentration (Fig. 3D). Additionally, Bcl-2 expression was opposite to KCNQ1OT1 expression in RGCs, while Bax presented with the same trend as KCNQ1OT1 expression (Fig. 3E-G). RGCs treated with 150 μM NMDA were used for subsequent experiments.

3.5. Suppressed KCNQ1OT1 is available to alleviate NMDA-induced suppression of RGC growth

Transfection of sh-KCNQ1OT1 or sh-NC into NMDA-treated RGCs aimed to explore KCNQ1OT1's impacts on RGCs, and the successful transfection was verified (Fig. 4A). Various experimental results illuminated that after KCNQ1OT1 was down-regulated, NMDA-treated RGCs showed the promotion of proliferation and anti-apoptosis abilities, the increase of Bcl-2 expression and the decrease of Bax expression (Fig. 4B-G). To sum up, NMDA restrained the growth of RGCs *in vitro*, while silenced KCNQ1OT1 was available to alleviate the influence of NMDA.

3.6. KCNQ1OT1 modulates HOXB3 via miR-93-5p

Test of miR-93-5p and HOXB3 expression in NMDA-treated RGCs was implemented, demonstrating that miR-93-5p was decreased while HOXB3 was elevated by NMDA dose-dependently (Fig. 5A-B). KCNQ1OT1 or HOXB3 and miR-93-5p had binding sites on the starBase (Fig. 5C-D). The relative luciferase activity was suppressed after co-transfection with KCNQ1OT1-WT or HOXB3-WT with miR-93-5p mimic (Fig. 5E-F), confirming that KCNQ1OT1 or HOXB3 had a targeting with miR-93-5p. Then, it was noticed that after silencing KCNQ1OT1, miR-93-5p expression was elevated, while HOXB3 expression was suppressed (Fig. 5G-H). In short, KCNQ1OT1 modulated HOXB3 via miR-93-5p.

3.7. Elevated miR-93-5p or suppressed HOXB3 is available to mitigate the repression of NMDA on RGC growth

To explore the impact of miR-93-5p or HOXB3 on RGCs, miR-93-5p mimic/mimic NC or si-HOXB3/NC was transfected into NMDA-treated RGCs, and the successful transfection was verified (Fig. 6A-B). Various experimental results illuminated that NMDA-induced impacts on proliferation, apoptosis, Bcl-2 and Bax expression in RGCs were alleviated by elevating miR-93-5p or silencing HOXB3 (Fig. 6C-H). In short, elevated miR-93-5p or silenced HOXB3 was available to alleviate the suppression of NMDA on RGC growth.

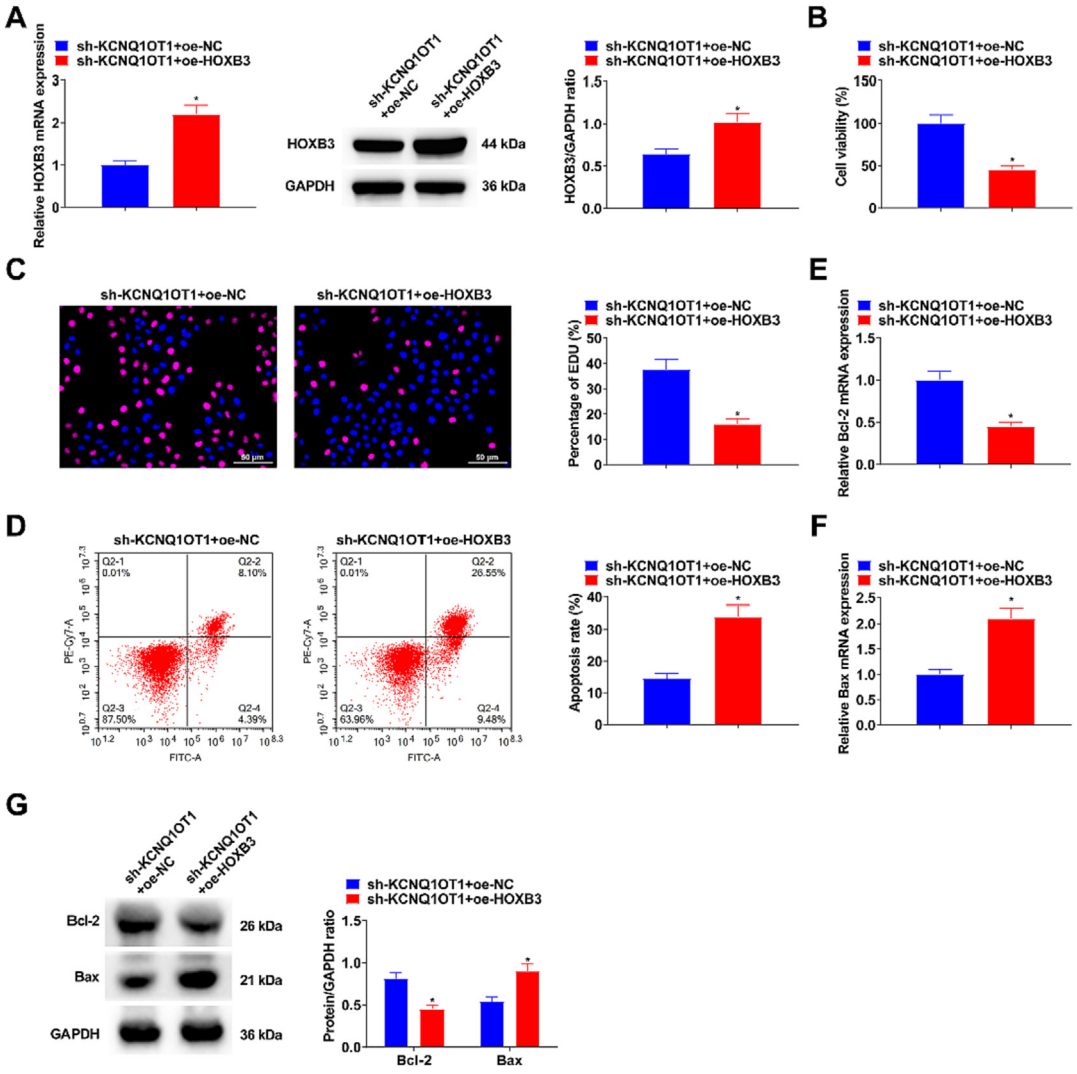

Fig. 7. Elevated HOXB3 is available to turn around silenced KCNQ1OT1's action. (A) RT-qPCR and Western blot test of HOXB3; (B) MTT detection of cell viability; (C) EDU examination of cell proliferation; (D) Flow cytometry test of cell apoptosis; (E-G) RT-qPCR and Western blot examination of Bcl-2 and Bax. The data in the figure are all measurement data in the form of mean ± SD. * vs. the sh-KCNQ1OT1+ oe-NC, $P < 0.05$.

3.8. Elevated HOXB3 is available to turn around the action of silenced KCNQ1OT1

To further verify the modulation of KCNQ1OT1/miR-93-5p/HOXB3 axis on RGCs, sh-KCNQ1OT1 + oe-HOXB3 and sh-KCNQ1OT1 + oe-NC were transfected into NMDA-treated RGCs. Elevated HOXB3 turned around the suppression of silenced KCNQ1OT1 on HOXB3 expression (Fig. 7A), as well as on RGC proliferation (Fig. 7B-C), apoptosis (Fig. 7D), Bcl-2 and Bax expression (Fig. 7E-G). In general, elevated HOXB3 was available to turn around the action of silenced KCNQ1OT1.

4. Discussion

Glaucoma is a crucial cause of blindness worldwide, but it is not detected until irreversible vision loss occurs, and its specific pathogenesis remains uncertain [20]. Presently, numerous studies have elucidated that the expression of multiple LncRNAs is aberrant in glaucoma patients and can be adopted as latent biomarkers for glaucoma [21]. In this study, it was first discovered that KCNQ1OT1 was elevated in glaucoma patients, and it was associated with glaucoma's clinicopathological indexes. Additionally, elevated KCNQ1OT1 was tested in both the NMDA-stimulated glaucoma rat model and the RGCs model. These results illuminated that KCNQ1OT1 was available to be adopted as a latent biomarker for glaucoma.

KCNQ1OT1 is located on human chromosome 11p15.5 and is linked with disease occurrence [22], such as some eye diseases [23]. Initially, KCNQ1OT1 was discovered to be associated with diversified pathophysiological mechanisms of diabetic complications like diabetic retinopathy and diabetic cardiomyopathy. Zhang et al. [24] have further discovered that KCNQ1OT1 participates in the pathological mechanism of diabetic endothelial cornea. Liu et al. [25] have discovered that repression of KCNQ1OT1 suppresses the activity, migration and epithelial mesenchymal transformation of human lens epithelial cells via miR-26a-5p/ITGAV/TGF-β/Smad3 axis. Jin et al. [26] have also disclosed that KCNQ1OT1 accelerates cataract occurrence via targeting miR-214 and activating caspase-1 pathway. In this research, KCNQ1OT1 expression was elevated in glaucoma patients, and it was negatively associated with PEDF and IL-12 and positively linked with Hcy and IL-4 contents. Serum PEDF, a multifunctional secretory protein, is provided with a latent neuroprotec-

tive effect in retinal diseases, while PEDF is elevated when IOP is elevated, and has the potential to immediately restrain RGC apoptosis [27]. Hcy, a neurotoxin, induces RGC apoptosis via stimulating NMDA receptor, and its elevation might lead to optic nerve damage in glaucoma [28]. IL-12 inhibits ganglion cell apoptosis and protects the optic nerve and IL-4 confers great impact on the process of optic nerve injury, and its high expression represents severe optic nerve injury [29,30]. The rising concentration of NMDA is available to stimulate the overactivation of its receptor (NMDAR), thus resulting in excitatory toxicity and RGC apoptosis, which is frequently adopted to construct glaucoma models [31]. Then, the glaucoma rat model and *in vitro* RGCs cell model were constructed to further explore KCNQ1OT1's action in glaucoma. It was discovered that *in vivo*, injection with NMDA damaged rat visual function, elevated IOP, accelerated RGCs apoptosis, and induced KCNQ1OT1 expression over time. Down-regulation of KCNQ1OT1 could improve visual impairment in glaucoma rats. *In vitro*, with the increase of NMDA concentration, KCNQ1OT1 expression in RGCs was gradually elevated. Additionally, after silencing KCNQ1OT1, NMDA-induced impacts on advancement capacity, Bcl-2 and Bax expression of RGCs were reduced.

miRNAs exert a crucial action in glaucoma occurrence and development [32]. An antecedent study has explored the miRNA profile in glaucoma optic neuropathy in all respects, and it was discovered that 88 miRNAs were differentially expressed between primary open-angle glaucoma (POAG) and cataract control eyes. There are 16 miRNAs with different expression signatures between POAG eyes with severe visual field injury and eyes with moderate visual field injury, covering miR-93-5p [33]. Li et al. [34] have further discovered that miR-93-5p modulates NMDA-induced RGC autophagy in glaucoma via the Akt/mammalian target of rapamycin (mTOR) pathway via targeting phosphatase and tensin homologue. In addition, miR-93-5p inhibits retinal neuronal apoptosis in acute ocular hypertension models by regulating PDCD4 [35]. In this research, miR-93-5p was downregulated in glaucoma, while elevated miR-93-5p was available to alleviate the repression of NMDA on RGC growth. Additionally, it was discovered that miR-93-5p acted in glaucoma via modulating HOXB3.

HOXB3, a member of the transcription factors HOX family covering homologous domains, has been testified to exert a critical role in embryogenesis, and it is provided with a complex mRNA, LncRNA and antisense RNA transcription profile [36]. All along, reports on HOXB3 have primarily explored its role in cancer, like cervical squamous cell carcinoma [37], colon cancer [38] and pancreatic cancer [39]. Presently, several studies have discovered that HOXB3 is also nearly associated with eye diseases. Tao et al. [40] have detected the ectopic expression of HOXB3 in orbital adipose stem cells of patients with thyroid-associated orbital diseases. MiR-7 lessens glucose-stimulated injury via HoxB3 and PI3K/Akt/mTOR pathways in retinal pigment epithelial cells [41]. In this research, it was discovered that HOXB3 was elevated in NMDA-treated RGCs. Elevated HOXB3 turned around the action of silenced KCNQ1OT1. These results elucidated that KCNQ1OT1/miR-93-5p/HOXB3 axis was a novel regulatory mechanism of glaucoma progression. However, this study also has shortcomings, that is, the clinical sample size is small, and our conclusions need to be further verified.

5. Conclusions

In brief, KCNQ1OT is elevated in the serum of glaucoma patients and can be adopted as a latent biomarker of glaucoma. Additionally, the results uncover the progression of KCNQ1OT to modulate glaucoma *in vivo* and *in vitro* via targeting the miR-93-5p/HOXB3 axis. Our research provides a new target for the treatment of glaucoma, and we hope to further explore the clinical application of KCNQ1OT in the future.

Ethical approval

The present study was approved by the Ethics and Scientific Committees of The First Affiliated Hospital of Gannan Medical College and performed in accordance with The Declaration of Helsinki. Written informed consent was obtained from all patients prior to the study start.

The present study was approved by the Animal experiments that were approved by The First Affiliated Hospital of Gannan Medical College and all procedures complied with the National Institutes of Health Guide for the Use of Laboratory Animals.

Author contributions

- Study conception and design: Z Xie
- Data collection: L Liu, H Wang
- Analysis and interpretation of results: H Zhang, J Liu
- Draft manuscript preparation: Z Xie
- Revision of the results and approval of the final version of the manuscript: H Zhang, H Wang, J Liu, L Liu, Z Xie.

Financial support

This research did not receive any specific grant from funding agencies in the public, commercial, or not-for-profit sectors.

Conflict of interest

The authors have no conflicts of interest to declare.

Supplementary material

https://doi.org/10.1016/j.ejbt.2023.10.002.

References

[1] Li C, Qiu G, Liu B, et al. Neuroprotective effect of lignans extracted from *Eucommia ulmoides* Oliv. on glaucoma-related neurodegeneration. Neurol Sci 2016;37(5):755–62. https://doi.org/10.1007/s10072-016-2491-3. PMid: 26829935.
[2] Youngblood H, Hauser M, Liu Y. Update on the genetics of primary open-angle glaucoma. Exp Eye Res 2019;188:. https://doi.org/10.1016/j.exer.2019.107795. PMid: 31525344107795.
[3] MacGregor S, Ong J, An J, et al. Genome-wide association study of intraocular pressure uncovers new pathways to glaucoma. Nat Genet 2018;50(8):1067–71. https://doi.org/10.1038/s41588-018-0176-y. PMid: 30054594.
[4] Jonas J, Aung T, Bourne R, et al. Glaucoma. Lancet 2017;390(10108):2183–93. https://doi.org/10.1016/S0140-6736(17)31469-1. PMid: 28577860.
[5] Garcia-Medina J, Garcia-Medina M, Garrido-Fernandez P, et al. A two-year follow-up of oral antioxidant supplementation in primary open-angle glaucoma: An open-label, randomized, controlled trial. Acta Ophthalmologica 2015;93(6):546–54. https://doi.org/10.1111/aos.12629. PMid: 25545196.
[6] Kopp F, Mendell J. Functional classification and experimental dissection of long noncoding RNAs. Cell 2018;172(3):393–407. https://doi.org/10.1016/j.cell.2018.01.011. PMid: 29373828.
[7] Wawrzyniak O, Zarębska Ż, Rolle K, et al. Circular and long non-coding RNAs and their role in ophthalmologic diseases. Acta Biochimica Polonica 2018;65(4):497–508. https://doi.org/10.18388/abp.2018_2639. PMid: 30428483.
[8] Li F, Wen X, Zhang H, et al. Novel insights into the role of long noncoding RNA in ocular diseases. Int J Mol Sci 2016;17(4):478. https://doi.org/10.3390/ijms17040478. PMid: 27043545.
[9] Li H, You Q, Xu L, et al. Long non-coding RNA-MALAT1 mediates retinal ganglion cell apoptosis through the PI3K/Akt signaling pathway in rats with glaucoma. Cell Physiol Biochem 2017;43(5):2117–32. https://doi.org/10.1159/000484231. PMid: 29065394.
[10] Lin Z, Long P, Zhao Z, et al. Long noncoding RNA KCNQ1OT1 is a prognostic biomarker and mediates CD8 T cell exhaustion by regulating CD155 expression in colorectal cancer. Int J Biol Sci 2021;17(7):1757–68. https://doi.org/10.7150/ijbs.59001. PMid: 33994860.

[11] Zhang M, Cheng K. Long non-coding RNA KCNQ1OT1 promotes hydrogen peroxide-induced lens epithelial cell apoptosis and oxidative stress by regulating miR-223-3p/BCL2L2 axis. Exp Eye Res 2021;206:. https://doi.org/10.1016/j.exer.2021.108543. PMid: 33744257108543.
[12] Li X, Jin X, Wang J, et al. Dexamethasone attenuates dry eye-induced pyroptosis by regulating the KCNQ1OT1/miR-214 cascade. Steroids 2022;186:. https://doi.org/10.1016/j.steroids.2022.109073. PMid: 35779698109073.
[13] Wang W, Du SL, Zhang XL. Corneal deformation response in patients with primary open-angle glaucoma and in healthy subjects analyzed by Corvis ST. Invest Ophthalmol Vis Sci 2015;56(9):5557–65. https://doi.org/10.1167/iovs.15-16926. PMid: 26305527.
[14] Zheng M, Zheng YL, Gao MM, et al. Expression and clinical value of lncRNA MALAT1 and lncRNA ANRIL in glaucoma patients. Exp Ther Med 2020;19(2):1329–35. https://doi.org/10.3892/etm.2019.8345.
[15] Lambuk L, Jafri AJA, Arfuzir NNN, et al. Neuroprotective effect of magnesium acetyltaurate against NMDA-induced excitotoxicity in rat retina. Neurotox Res 2017;31(1):31–45. https://doi.org/10.1007/s12640-016-9658-9. PMid: 27568334.
[16] Luo X, Yu Y, Xiang Z, et al. Tetramethylpyrazine nitrone protects retinal ganglion cells against *N*-methyl-D-aspartate-induced excitotoxicity. J Neurochem 2017;141(3):373–86. https://doi.org/10.1111/jnc.13970. PMid: 28160291.
[17] Kroeber M, Davis N, Holzmann S, et al. Reduced expression of Pax6 in lens and cornea of mutant mice leads to failure of chamber angle development and juvenile glaucoma. Hum Mol Genet 2010;19(17):3332–42. https://doi.org/10.1093/hmg/ddq237 PMid: 20538882.
[18] Gao F, Li T, Hu J, et al. Comparative analysis of three purification protocols for retinal ganglion cells from rat. Mol Vis 2016;22:387–400. PMid: 27122968.
[19] Lin B, Koizumi A, Tanaka N, et al. Restoration of visual function in retinal degeneration mice by ectopic expression of melanopsin. Proc Natl Acad Sci USA 2008;105(41):16009–14. https://doi.org/10.1073/pnas.0806114105. PMid: 18836071.
[20] Hindle A, Thoonen R, Jasien J, et al. Identification of candidate miRNA biomarkers for glaucoma. Invest Ophthalmol Vis Sci 2019;60(1):134–46. https://doi.org/10.1167/iovs.18-24878 PMid: 30629727.
[21] Zhang F, Zhao Y, Cao M, et al. The potential role of long noncoding RNAs in primary open-angle glaucoma. Graefe's Arch Clin Experimental Ophthalmol 2021;259:3805–14. https://doi.org/10.1007/s00417-021-05279-w. PMid: 34244823.
[22] Chen B, Ma J, Li C, et al. Long noncoding RNA KCNQ1OT1 promotes proliferation and epithelial-mesenchymal transition by regulation of SMAD4 expression in lens epithelial cells. Mol Med Rep 2018;18(1):16–24. https://doi.org/10.3892/mmr.2018.8987.
[23] Yao L, Yang L, Song H, et al. MicroRNA miR-29c-3p modulates FOS expression to repress EMT and cell proliferation while induces apoptosis in TGF-β2-treated lens epithelial cells regulated by lncRNA KCNQ1OT1. Biomed Pharmacother 2020;129:. https://doi.org/10.1016/j.biopha.2020.110290. PMid: 32534225110290.
[24] Zhang Y, Song Z, Li X, et al. Long noncoding RNA KCNQ1OT1 induces pyroptosis in diabetic corneal endothelial keratopathy. Am J Physiol Cell Physiol 2020;318(2):C346–59. https://doi.org/10.1152/ajpcell.00053.2019. PMid: 31693400.
[25] Liu J, Dong Y, Wen Y, et al. LncRNA KCNQ1OT1 knockdown inhibits viability, migration and epithelial-mesenchymal transition in human lens epithelial cells via miR-26a-5p/ITGAV/TGF-beta/Smad3 axis. Exp Eye Res 2020;200:. https://doi.org/10.1016/j.exer.2020.108251. PMid: 32950535108251.
[26] Jin X, Jin H, Shi Y, et al. Long non-coding RNA KCNQ1OT1 promotes cataractogenesis via miR-214 and activation of the caspase-1 pathway. Cell Physiol Biochem 2017;42(1):295–305. https://doi.org/10.1159/000477330. PMid: 28535504.
[27] Bürger S, Meng J, Zwanzig A, et al. Pigment Epithelium-Derived Factor (PEDF) receptors are involved in survival of retinal neurons. Int J Mol Sci 2020;22(1):369. https://doi.org/10.3390/ijms22010369. PMid: 33396450.
[28] Roedl J, Bleich S, Reulbach U, et al. Homocysteine levels in aqueous humor and plasma of patients with primary open-angle glaucoma. J Neural Transm 2007;114(4):445–50. https://doi.org/10.1007/s00702-006-0556-9. PMid: 16932990.
[29] Benitez-Del-Castillo J, Cantu-Dibildox J, Sanz-González SM, et al. Cytokine expression in tears of patients with glaucoma or dry eye disease: A prospective, observational cohort study. Eur J Ophthalmol 2019;29(4):437–43. https://doi.org/10.1177/1120672118795399. PMid: 30175615.
[30] Aketa N, Yamaguchi T, Suzuki T, et al. Iris damage is associated with elevated cytokine levels in aqueous humor. Invest Ophthalmol Vis Sci 2017;58(6):BIO42–51. https://doi.org/10.1167/iovs.17-21421. PMid: 28475702.
[31] Lambuk L, Iezhitsa I, Agarwal R, et al. Antiapoptotic effect of taurine against NMDA-induced retinal excitotoxicity in rats. Neurotoxicology 2019;70:62–71. https://doi.org/10.1016/j.neuro.2018.10.009. PMid: 30385388.
[32] Guo R, Shen W, Su C, et al. Relationship between the pathogenesis of glaucoma and miRNA. Ophthalmic Res 2017;57(3):194–9. https://doi.org/10.1159/000450957. PMid: 28073110.
[33] Liu Y, Chen Y, Wang Y, et al. microRNA profiling in glaucoma eyes with varying degrees of optic neuropathy by using next-generation sequencing. Invest Ophthalmol Vis Sci 2018;59(7):2955–66. https://doi.org/10.1167/iovs.17-23599. PMid: 30025119.
[34] Li R, Jin Y, Li Q, et al. MiR-93-5p targeting PTEN regulates the NMDA-induced autophagy of retinal ganglion cells via AKT/mTOR pathway in glaucoma. Biomed Pharmacother 2018;100:1–7. https://doi.org/10.1016/j.biopha.2018.01.044. PMid: 29421576.
[35] Tan C, Shi W, Zhang Y, et al. MiR-93-5p inhibits retinal neurons apoptosis by regulating PDCD4 in acute ocular hypertension model. Life Science Alliance 2023;6(9):. https://doi.org/10.26508/lsa.202201732. PMid: 37308277e202201732.
[36] Chan K, Qi J, Sham M. Multiple coding and non-coding RNAs in the *Hoxb3* locus and their spatial expression patterns during mouse embryogenesis. Biochem Biophys Res Commun 2010;398(2):153–9. https://doi.org/10.1016/j.bbrc.2010.05.150 PMid: 20515659.
[37] Liu X, Shen X, Zhang J. Long non-coding RNA LINC00514 promotes the proliferation and invasion through the miR-708-5p/HOXB3 axis in cervical squamous cell carcinoma. Environ Toxicol 2021;37(1):161–70. https://doi.org/10.1002/tox.23387. PMid: 34652879.
[38] Cui M, Chen M, Shen Z, et al. LncRNA-UCA1 modulates progression of colon cancer through regulating the miR-28-5p/HOXB3 axis. J Cell Biochem 2019;120(5):6926–36. https://doi.org/10.1002/jcb.27630. PMid: 30652355.
[39] Yang D, Yan R, Zhang X, et al. Deregulation of MicroRNA-375 inhibits cancer proliferation migration and chemosensitivity in pancreatic cancer through the association of HOXB3. Am J Transl Res 2016;8(3):1551–9. PMid: 27186281.
[40] Tao W, Ayala-Haedo J, Field M, et al. RNA-sequencing gene expression profiling of orbital adipose-derived stem cell population implicate *HOX* genes and WNT signaling dysregulation in the pathogenesis of thyroid-associated orbitopathy. Investig. Ophthalmol Vis Sci 2017;58(14):6146–58. https://doi.org/10.1167/iovs.17-22237. PMid: 29214313.
[41] Yang Z, Hu H, Zou Y, et al. miR-7 Reduces high glucose induced-damage via HoxB3 and PI3K/AKT/mTOR signaling pathways in retinal pigment epithelial cells. Curr Mol Med 2020;20(5):372–8. https://doi.org/10.2174/1566524019666191023151137. PMid: 31702491.